Synthesis of cuprous oxide nanocubes combined with chitosan nanoparticles and its application to p-nitrophenol degradation

Tran Thi Bich Quyen[1*], Ngo Nguyen Tra My[1], Do Thi Thuy Ngan[1], Duy Toan Pham[2], Doan Van Hong Thien[1]

[1]Department of Chemical Engineering, College of Technology, Can Tho University, 3/2 Street, Ninh Kieu District, Can Tho City, Viet Nam
[2]Department of Chemistry, College of Natural Sciences, Can Tho University, 3/2 Street, Ninh Kieu District, Can Tho 900000, Viet Nam

*Author to whom correspondence should be addressed:

Tran Thi Bich Quyen

Can Tho University, Viet Nam
ttbquyen@ctu.edu.vn
ORCID: 0000-0002-9304-5544

accepted manuscript

This article has been accepted for publication and undergone full peer review but has not been through the copyediting, typesetting, and proofreading process, leading to differences between this version and the official version of record.

Please cite this article as Tran T.B.Q., Ngo N.T.M., Do T.T.N., Duy T.P., Doan V.H.T. Synthesis of cuprous oxide nanocubes combined with chitosan nanoparticles and its application to p-nitrophenol degradation. *Mongolian Journal of Chemistry,* **22**(48), 2021, xx-xx
doi.org/10.5564/mjc.v22i48.1564

Synthesis of cuprous oxide nanocubes combined with chitosan nanoparticles and its application to *p*-nitrophenol degradation

Tran Thi Bich Quyen[1*], Ngo Nguyen Tra My[1], Do Thi Thuy Ngan[1], Duy Toan Pham[2], Doan Van Hong Thien[1]

[1]Department of Chemical Engineering, College of Technology, Can Tho University, 3/2 Street, Ninh Kieu District, Can Tho City, Vietnam

[2]Department of Chemistry, College of Natural Sciences, Can Tho University, 3/2 Street, Ninh Kieu District, Can Tho 900000, Vietnam

ABSTRACT

For the first time, cuprous oxide nanocubes (Cu_2O NCBs) were successfully combined with chitosan nanoparticles (CS NPs) to generate Cu_2O NCBs/CS NPs composites material with highly optical property and photocatalytic activity using a simple and eco-friendly synthetic approach at room temperature for 30 min. The synthesized Cu_2O NCBs/CS NPs were characterized by Ultraviolet-visible spectroscopy (UV-vis), Fourier transform infrared spectroscopy (FTIR), X – ray Diffraction (XRD), Transmission Electron Microscope (TEM) and Energy-dispersive X-ray spectroscopy (EDX). Results show that the Cu_2O NCBs/CS NPs composites possessed an average particle size of ~3-5 nm; in which, Cu_2O had the form of nanocubes with a size of ~3-4 nm and CS NPs had spherical shape with a size of ~4-5 nm. In addition, the composition percentages of elements presented in Cu_2O NCBs/CS NPs composites material were: Cu (23.99%), O (38.18%), and C (33.61%). Moreover, Cu_2O NCBs/CS NPs composites material was also investigated for photocatalytic activity applied in p-nitrophenol degradation. The obtained results showed that the catalytic capability of Cu_2O NCBs/CS NPs for p-nitrophenol reduction reached the highest efficiency of >55% in the treatment time of 25 min, and this efficiency was higher than that of the ZnO@chitosan nanoparticles catalyst under the same conditions.

Keywords: Cuprous oxide nanocubes, chitosan nanoparticles, cuprous oxide nanocubes/chitosan nanoparticles composites, photocatalytic activity, p-nitrophenol.

accepted manuscript

INTRODUCTION

As a side effect of industrialization, many polluting compounds were discharged into the environment, especially the water environment. To this end, p-Nitrophenol (p-NP) is one of the most refractory and stable nitroaromatic compounds due to its resistance to chemical and biological degradation [1]. This organic toxic is widely used in the synthesis of plenty of industrial and agricultural products such as pesticides, herbicides, petrochemicals, explosives, pharmaceuticals, and dyes [2-4]. p-NP contamination has significant effects on human and animal health. Thus, p-NP was listed as one of the priority hazardous and toxic pollutants by the U.S. Environmental Protection Agency (EPA) [5]. Various studies have been performed to reduce the content of p-NP in solution, such as photocatalytic hydrogenation [1, 6], photoelectrocatalytic [7, 8], biological degradation [9], and metal-free catalyst [10]. In recent years, the reduction of p-NP to p-aminophenol (p-AP) has gained attention from the scientific community, since p-AP is a low toxic compound useful as an important intermediate in the preparation of pharmaceuticals, lubricants, and dyes [11].

Obviously, metal oxide-based semiconductor nanomaterials have received much attention due to their excellent physical and chemical properties, which can be applied in various practical fields. In particular, cuprous oxide (Cu_2O) is considered an important p-type semiconductor material because of its attractive optical properties. The bandgap energy of Cu_2O is between 1.95-2.2 eV [12]. Therefore, it represents a promising candidate for many applications such as photovoltaic, sensors, superconductors, and especially, photocatalysis [13]. The photocatalytic ability of Cu_2O has been extensively researched the removal of pollutants from aqueous medium such as methyl orange [9], methyl blue [10], brilliant red X-3B [11], and p-NP [12, 13]. Up to now, various studies have been devoted to the synthesis of Cu_2O nanoparticles (NPs) that adopt various morphologies such as: nanocubes [14], octahedra [14, 15], spherical particles [16], and nanowires [17]. The catalytic ability of Cu_2O is influenced by its morphology since the structure-related band gap energy is essential to their photocatalytic performance [7]. The photocatalytic activity of pure Cu_2O is very low because of the easy recombination between photo-generated electrons and holes, be oxidized or easy to aggregate to micron-size [11]. Several methods including the incorporation of Cu_2O composites with noble metal [18] and other semiconductors [19] have been developed to enhance the photocatalytic activity of pure Cu_2O under visible-light radiation. In this work, a substrate

accepted manuscript

that is able to disperse and stabilize the Cu_2O NPs and enhance its photocatalytic performance has been proposed. Chitosan (CS) is one of the most commonly used natural biopolymers [20]. CS is an abundant low-cost raw material with high reproducibility and biodegradability [21]. CS NPs possess surface and interface effect, small size and quantum size effect [22]. In addition, CS NPs can be easily combined with metal ions or metal oxides to form composites (due to the existence of $-NH_2$ and -OH functional groups in the molecule). These composites have a stable structure and shape and higher photocatalytic activity than the original metal oxide properties [23].

To the best of our knowledge, there have been no published reports concerning the synthesis of a composite material comprised of both Cu_2O nanocubes and chitosan nanoparticles (denoted here as Cu_2O NCBs/CS NPs). Herein, Cu_2O NCBs were successfully synthesized and combined with CS NPs to generate Cu_2O NCBs/CS NPs composites by a rapid and simple method. Besides, the properties characterizations of this nanocomposites material have also been analyzed. Moreover, the synthesized Cu_2O NCBs/CS NPs nanocomposites have been used as a catalyst material for the degradation of p-nitrophenol.

EXPERIMENTAL

Materials: Copper sulfate ($CuSO_4.5H_2O$; 99.5%), Sodium borohydride ($NaBH_4$; 99%), Sodium hydroxide (NaOH; 99%), and Hydrazine hydrate ($N_2H_4.2H_2O$; 99%) were purchased from Sigma-Aldrich (Merck). Acetic acid (CH_3COOH; 99%) and D-glucose ($C_6H_{12}O_6.H_2O$, 99.5%) were bought from Hemidia, India. Chitosan of Vietnam; and p-Nitrophenol ($C_6H_5NO_3$, 99%) was purchased from Dengfeng Chemical Technology Co., Ltd,. All solutions were prepared with deionized water (DI H_2O) from a MilliQ system.

Preparation of cuprous oxide nanocubes (Cu_2O NCBs): Typically, 70.30 mg of $CuSO_4.5H_2O$ and 0.361 g of D-Glucose were dissolved in 100 mL of deioned water (DI H_2O) under vigorous stirring. After 15 min, 100 μL of NaOH (10 M) was added dropwise into the copper sulfate solution and stirred for 15 min. Then, 200 μL of $N_2H_4.2H_2O$ (2 M) was added into the mixture and continuous stirred for 20-30 min. As a result, the solution color changed from blue to orange-red. Finally, the prepared-solution was centrifuged and washed several times with DI H_2O to neutral pH and re-dispersed in 15 mL of DI H_2O to use for next steps.

Preparation of chitosan nanoparticles (CS NPs: 1 g of chitosan (CS) was added into 100 mL of acetic acid (0.5% in DI H_2O) and stirred at 60°C for 1 h. Then, 10 mL of

accepted manuscript

sodium triphosphate (STPP) (1 mg/mL in DI H_2O) was mixed with as-prepared CS solution and stirred for 30 min. Finally, the prepared CS NPs solution was centrifuged and washed three times with DI H_2O to obtain CS NPs with high purity and dispersed in 100 mL of DI H_2O to use for next experiments.

Synthesis of Cu_2O NCBs/CS NPs composites: To formulate Cu_2O NCBs/CS NPs composites material, the prepared CS NPs was added to Cu_2O NCBs solution. Various volumes of CS NPs solution of respective: 100 μL; 200 μL; 500 μL; and 1000 μL was added dropwise into 5 mL of Cu_2O NCBs solution and stirred at room temperature for 30 min to obtain Cu_2O NCBs/CS NPs composites material. This Cu_2O NCBs/CS NPs composite will be used as a photocatalyst material for p-nitrophenol degradation.

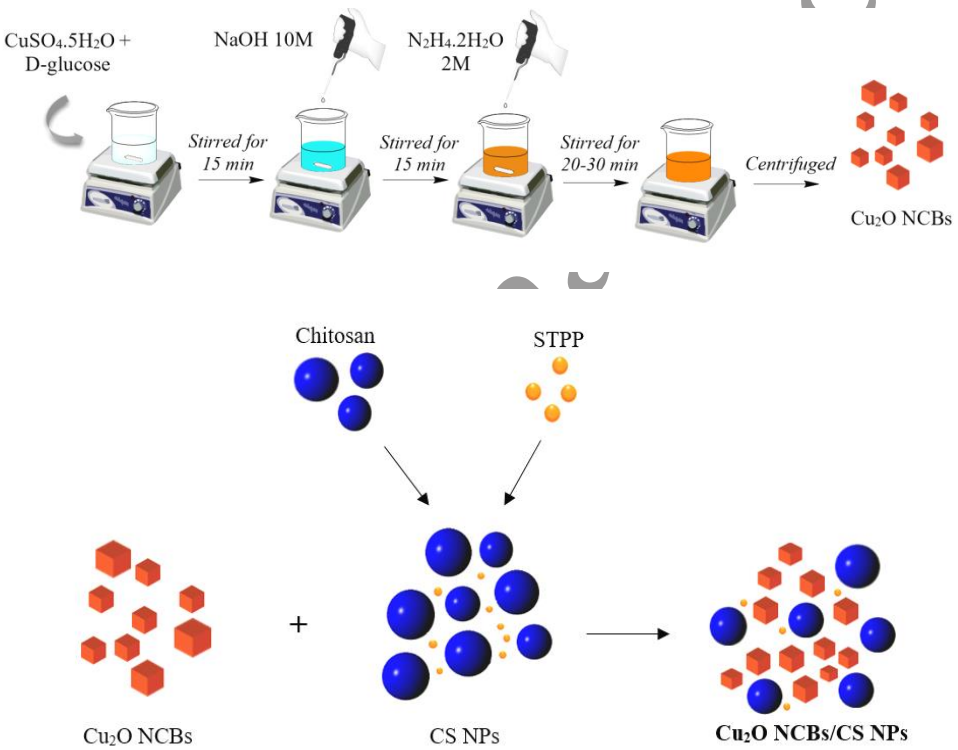

Scheme 1. Synthesis of Cu_2O NCBs/CS NPs nanocomposites

Catalytic activity test of Cu_2O NCBs/CS NPs composites: 30 μL of $NaBH_4$ (3 M) and 750 μL of p-nitrophenol (p-NP) (25 ppm) were stirred in the dark for 10 min to obtain the adsorption-desorption equilibrium. Then, under UV light (395 nm, OEM, Philips), 1.5 mL of Cu_2O NCBs/CS NPs (0.22 mg of Cu_2O NCBs loading) was added to the prepared-solution under constant stirring. The reaction was determined as soon as the catalyst was added into the solution. Consequently, the material treatment was separated by centrifugation within 2 min. On the other hand, an experiment to investigate the

reduction of p-NP by $NaBH_4$ in the absence of catalyst material was also performed for comparison. The amount of lost p-NP was determined according to Equation 1.

126

$$H\% = 100.(\Delta C/C_0) \quad (1)$$

Where $\Delta C = C_0 - C$ with C_0 and C are the initial and final concentrations of p-
129 nitrophenol, respectively.

Instrumentation: The Cu_2O NCBs/CS NPs synthesis process was observed by
132 recording the absorbance spectra between 200 and 900 nm on the UV-vis spectrophotometer (Thermo Scientific Evolution 60S UV-Vis spectrophotometer, USA). X-ray diffraction (XRD) was performed on a D8-Advance machine (Bruker, Germany) in
135 the 2θ range of 10°-80°. The Fourier transform infrared (FT-IR) spectra were obtained by Perkin Elmer Frontier MIR/NIR (Perkin Elmer, USA) in the range of 4000-400 cm^{-1}. Transmission electron microscopy (TEM) characterization was performed on a
138 Jem1010 device (Joel Company, Japan). Chemical properties and constituent components were analyzed via Energy-dispersive X-ray spectroscopy (EDX H-7593, Horiba, England).

141

RESULTS AND DISCUSSION

***Characterization and morphology of Cu_2O NCBs/CS NPs composites*:** Figure 1
144 shows the UV-vis result of the synthesized Cu_2O NCBs/CS NPs composites with various volumes of CS NPs solution. Obviously, the amount of CS NPs influenced the synthesis of Cu_2O NCBs/CS NPs composites. Figure 1A(a),(b) indicate that the initial
147 characteristic peak at 470 nm of Cu_2O NCBs shifted to the peak at 500 nm and 480 nm with higher absorption intensity corresponding to the added volume of CS NPs solution of 100 µL and 200 µL, respectively. Moreover, the absorption band in the range from
150 550 nm to 900 nm of Cu_2O NCBs tends to increase strongly (Figure 1A). Besides, a band gap with energy level at 2.08 eV of the synthesized Cu_2O NCBs was converted to 2.04 eV when combined with 200 µL of CS NPs solution – as shown in Figure 1B.
153 Therefore, it can be confirmed that CS NPs have the ability to enhance the optical properties of Cu_2O NCBs.

When the volume of CS NPs solution is excessive, the UV spectra showed the gradual
156 decrease and disappearance of the characteristic peak and optical absorption band of composites material (Figure 1A(d),(e)). Due to the interaction between the excess acid

accepted manuscript

in the CS NPs solution with Cu_2O NCBs to form Cu^{2+} ion or nano Cu, leading to a significant loss of Cu_2O NCBs, thereby making the optical absorbance of the material decreased. Thus, the volume of CS NPs solution at 200 µL was chosen as the optimal condition for the combination of CS NPs with Cu_2O NCBs to generate Cu_2O NCBs/CS NPs composites.

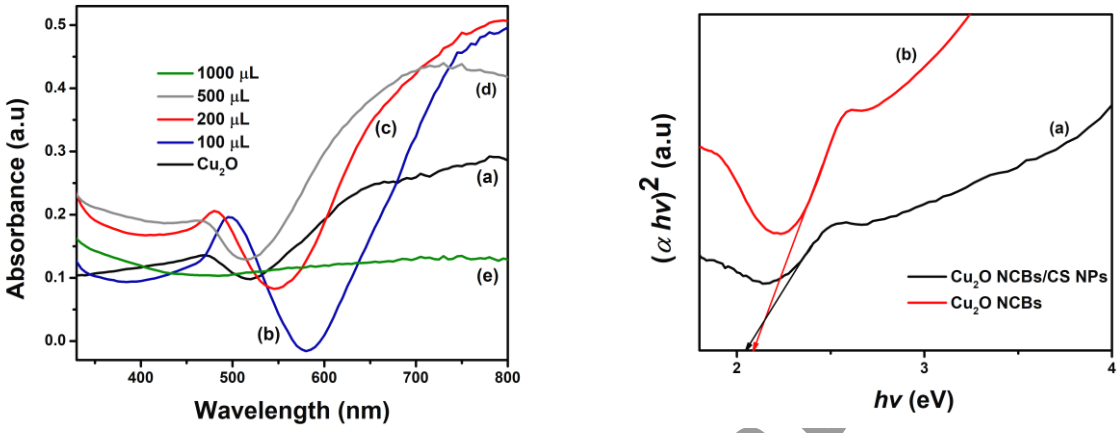

Fig. 1. **(A)** UV-Vis spectra of (a) Cu_2O nanocubes (Cu_2O NCBs) and Cu_2O NCBs/CS NPs composites with different volumes of CS NPs: (b) 100 µL; 200 µL; 500 µL; and 1000 µL. **(B)** Graphical determination of direct optical band gap of (a) Cu_2O NCBs/CS NPs and (b) Cu_2O NCBs, respectively.

To study the structure of Cu_2O NCBs/CS NPs composites, the FTIR spectra of pure CS NPs and composites were applied (Figure 2). The FTIR spectra of the obtained CS NPs showed characteristic oscillations at 3414 cm^{-1} and 2926 cm^{-1}, attributed to the stretching vibration of -NH_2, -OH, and aliphatic -CH_2 and -CH_3 groups, respectively [24]. The vibration bands at 1641 cm^{-1} and 1087 cm^{-1} are corresponding to the bending vibrations of -NH and -OH groups.

The transformation of chemical groups in CS NPs when forming of Cu_2O NCBs/CS NPs composites was shown in Figure 2(a). The broad absorption band between 3150-3414 cm^{-1} became a sharp peak at 3428 cm^{-1} due to the compression of the -OH group, possibly caused by the water molecule adsorbed on the surface of Cu_2O NCBs. Additionally, the peaks at 1641 cm^{-1} and 1087 cm^{-1} were shifted to 1611 cm^{-1} and 1060 cm^{-1}, respectively, indicating that the amine functional group (-NH) and the hydroxyl group (-OH) participated in the complexation process [25]. At the same time, the narrow oscillation range from 1450-1300 cm^{-1}, which was attributed to the fluctuation of C-N bonding in CS NPs and appeared with a sharp peak at 1411 cm^{-1} in FTIR spectra of Cu_2O NCBs/CS NPs. Besides, the characteristic absorption bands of Cu_2O NCBs were

accepted manuscript

shown at 720 cm^{-1} and 618 cm^{-1} [7]. The bands shift in the region from 1700-700 cm^{-1} is influenced by the absorption peak of Cu-O bonds in this region [15]. As a result, the maximum absorption peak intensity of Cu_2O NCBs/CS NPs composites are significantly changed compared to the pure CS NPs. This result was due to the strong surface interaction between CS NPs and Cu_2O NCBs.

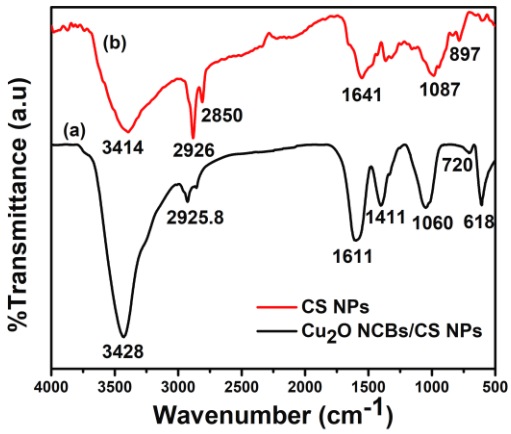

Fig. 2. FTIR spectra of (a) Cu_2O NCBs/CS NPs composites and (b) CS NPs, respectively.

The X-ray diffraction (XRD) results of CS NPs and Cu_2O NCBs/CS NPs composites are clearly shown in Figure 3. Figure 3(a) shows that there are a large amounts of hydroxyl and amino groups in the structure of CS NPs. The presence of STPP induces cross-links in CS circuits to form CS NPs with amorphous structure. This result is in complete agreement with a previous work [26]. The synthesized CS NPs structure improves metal ions absorption ability of CS NPs [27].

When CS NPs was added to the Cu_2O NCBs (Figure 3(b)), the characteristic diffraction peaks of Cu_2O were identified at six clear peaks with 2θ values of 29.5°; 38°; 42.1°; 53.2°; 70°; and 76.18°, corresponding to the crystal planes (110); (111); (200); (211); (311); and (222). These diffraction peaks completely coincide with the Cu_2O NCBs structure (JCPDS Card No. 05-0667) [28]. In addition, no other diffraction peaks arising from possible impurities such as Cu, CuO or $Cu(OH)_2$ were detected, thus, confirming the formation of pure Cu_2O NPs [24]. The increase in the intensity of the diffraction peak between Cu_2O NCBs/CS NPs composites and CS NPs was caused by diffraction/interlacing between the amorphous structure of CS NPs and the crystal structure of Cu_2O NCBs. This change of CS NPs represents a successful

accepted manuscript

210 interaction/binding between CS NPs and Cu_2O NCBs to form Cu_2O NCBs/CS NPs composites.

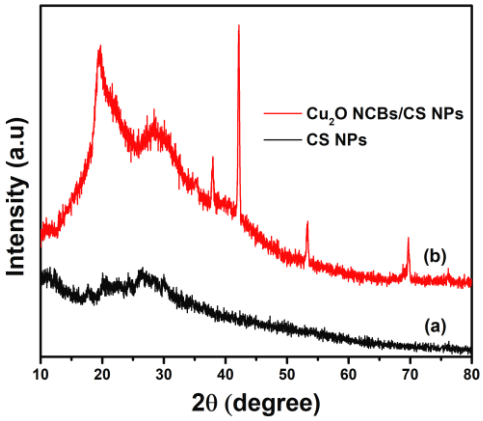

213 Fig. 3. X-ray diffraction (XRD) patterns of (a) CS NPs and (b) Cu_2O NCBs/CS NPs composites, respectively.

216 The morphology and size of the product was studied by TEM, Figure 4(a). The result shows that Cu_2O NCBs have the cubic structure with an average particle size ~3-4 nm; and CS NPs have spherical shape with an average particle size ~4-5 nm. Thus, the 219 synthesized Cu_2O NCBs/CS NPs composites have an average particle size of ~3-5 nm (Figure 4(b)). Additionally, the Cu_2O NCBs/CS NPs composites particles were uniformly distributed and dispersed without agglomeration.

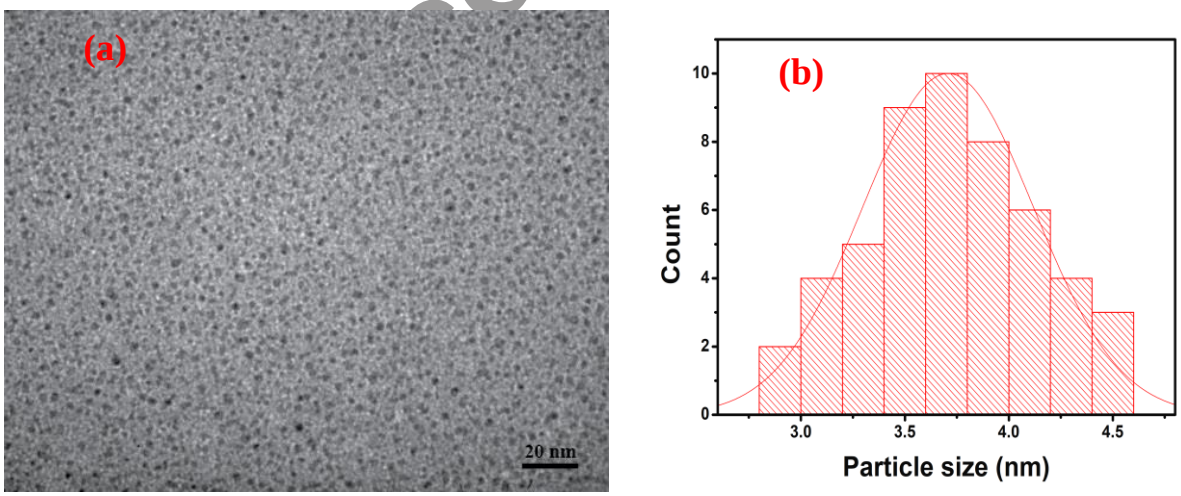

222 Fig. 4. (a) TEM image of Cu_2O NCBs/CS NPs composites and (b) Particle size distribution of Cu_2O NCBs/CS NPs composites, respectively.

225

EDX analysis was used to determine the composition of the synthesized Cu_2O NCBs/CS NPs composites sample. Figure 5 shows that the Cu_2O NCBs/CS NPs

ed manuscript

composites comprised elemental compositions including Cu (23.99%), O (38.18%), C (33.61%), and other elements like N and P. These results indicated that the presence of Cu_2O NCBs and CS NPs in the synthesized Cu_2O NCBs/CS NPs nanocomposites sample.

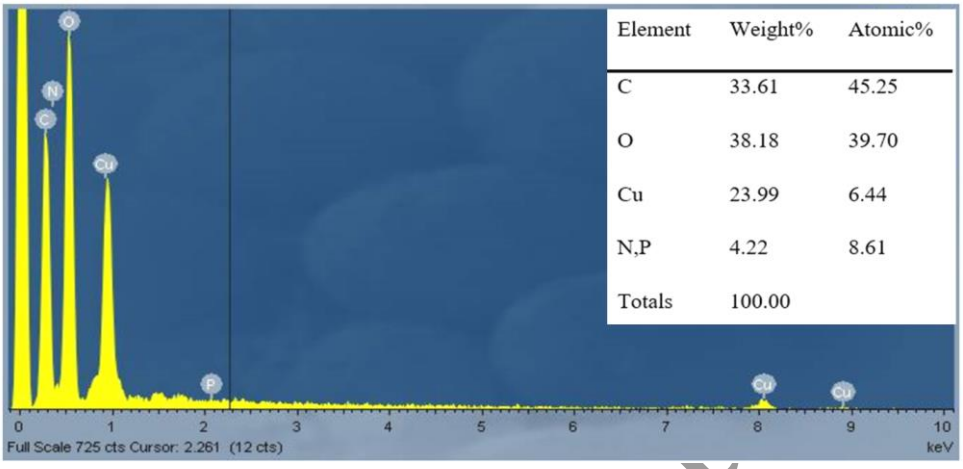

Element	Weight%	Atomic%
C	33.61	45.25
O	38.18	39.70
Cu	23.99	6.44
N,P	4.22	8.61
Totals	100.00	

Fig. 5. Energy dispersive X-ray (EDX) spectra of Cu_2O NCBs/CS NPs composites.

Photocatalytic activity of Cu_2O NCBs/CS NPs composites for p-nitrophenol degradation: The reduction of p-NP by $NaBH_4$ without using photocatalytic is presented in Figure 6. Firstly, the UV-vis spectrum (Figure 6(a)) indicated that the absorption wavelength of the initial p-NP was shifted from 317 to 400 nm immediately upon the addition of $NaBH_4$, corresponding to a significant change in solution color from light yellow to yellow-green due to the formation of 4-nitrophenolate ion. The reduction of p-NP by $NaBH_4$ is thermodynamically feasible but possesses a high kinetic impediment between negative ions that repel each other between p-nitrophenolate and BH_4^- in the absence of an effective catalyst [29, 30]. As shown in Figure 6(c), the yellow-green decolorization of the p-NP solution after 6 h has no significant change compared to that at the initial time. The decomposition percentage of p-NP after 6 h in the absence of catalyst was only 3.68%. This represented an extremely slow reaction rate in the absence of a catalyst.

accepted manuscript

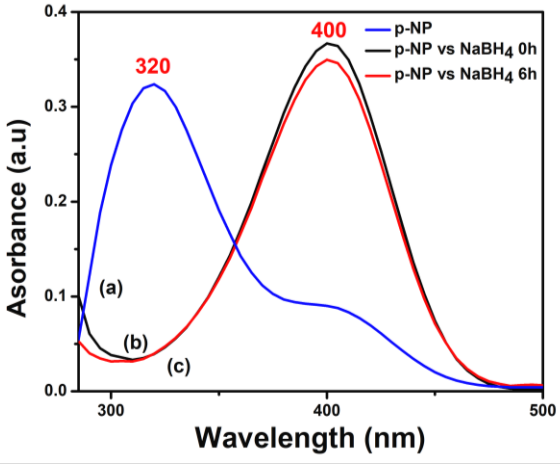

Fig. 6. UV-vis spectra of p-nitrophenol (p-NP) reduction without photocatalysts.

Using different catalysts in this reaction could yield disparate results due to the fact that many oxides are also unable to degrade p-NP under different reaction conditions [29]. In the presence of Cu_2O NCBs/CS NPs composites catalyst, the results of p-NP degradation (Figure 7) are significantly different from those of $NaBH_4$ without catalytic materials. The absorption peak at 400 nm of p-nitrophenolate ions was gradually decreased in intensity. At the same time, there was the formation and intensification of another absorption peak at 300 nm, which is the characteristic absorption peak of p-aminophenol (p-AP). Therefore, it is demonstrated that there was a conversion from p-NP to p-AP in the presence of Cu_2O NCBs/CS NPs. Meanwhile, the color of the solution also showed that p-NP was reduced in the reaction, the characteristic yellow color of p-nitrophenolate ion was lost and changed to a clear solution of p-AP. Indeed, the results of the graph in Figure 8 show that in the presence of Cu_2O NCBs/CS NPs photocatalysts, the higher the reaction time, the greater the percentage loss of p-nitrophenolate ions. The percentage (%) of p-NP decomposition in 1 min was 37.92%. After 25 min, this value was ~55.72% (Figure 8). Thus, it is confirmed that the positive charges on the Cu_2O NCBs/CS NPs composites' surfaces facilitated the interaction between nitrophenolate and BH_4^- ions. At the same time, the inactivity of ZnO@CS NPs in this reaction can be attributed to the absence of the electron relay process. In addition, the bandgap energy of Cu_2O NCBs/CS NPs (2.04 eV) is lower than that of ZnO@CS NPs (3.06 eV) and the existence of copper (Cu) metal on the surface of Cu_2O NCBs made the electron transfer occur faster. This result was completely consistent with previous studies [29].

accepted manuscript

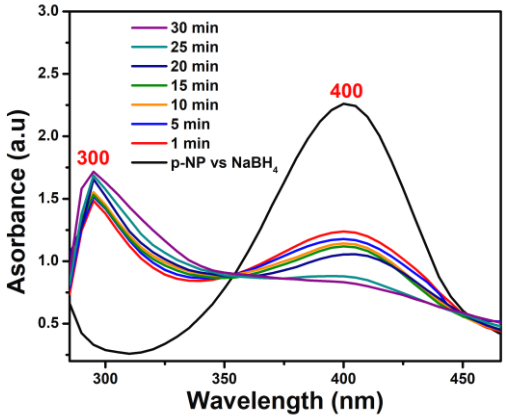

Fig. 7. UV-vis spectra of p-nitrophenol reduction with various reaction times using Cu_2O NCBs/CS NPs composites as a photocatalyst material.

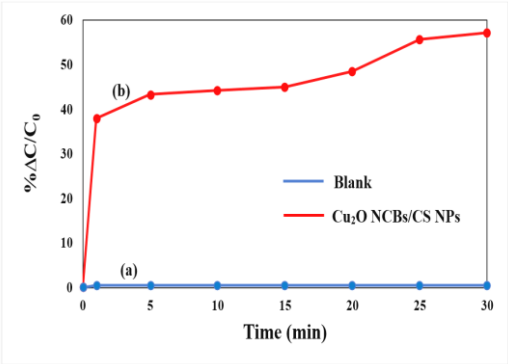

Fig. 8. Decomposition percent versus reaction time for the reduction of p-NP over (a) blank sample without catalyst and (b) using Cu_2O NCBs/CS NPs composites catalyst, respectively.

CONCLUSIONS

Cu_2O NCBs/CS NPs composites have been successfully synthesized by simple physical mixing between Cu_2O NCBs and CS NPs at room temperature for 30 min. Cu_2O NCBs/CS NPs composites have an average particle size ~3-5 nm; in which Cu_2O NCBs have the form of cubic particles (Cu_2O nanocubes – Cu_2O NCBs) with a dimension of ~3-4 nm and CS NPs have a spherical shape with a particle size of ~4-5 nm. Besides, the percent (%) composition of elements presented in Cu_2O NCBs/CS NPs composites material is as followed: Cu (23.99%), O (38.18%), C (33.61%) and other elements. Furthermore, the Cu_2O NCBs/CS NPs composite is confirmed as a potential and promising photocatalyst material for p-nitrophenol reduction with a treatment efficiency of >55% at a treatment time of 25 min. Thus, this study has

accepted manuscript

proposed a cheap nanocomposites catalyst instead of an expensive noble material system in the treatment of p-nitrophenol for the environmental problems.

REFERENCES

1. Zelekew O.A., Kuo D. (2016) A two-oxide nanodiode system made of double-layered p-type Ag_2O@n-type TiO_2 for rapid reduction of 4-nitrophenol, *Physical Chemistry Chemical Physics, 18(6)*, 4405-4414. https://doi.org/10.1039/C5CP07320K
2. Kulkarni M., Chaudhari A. (2007) Microbial remediation of nitro-aromatic compounds: an overview, *Journal of Environmental Management, 85(2)*, 496-512. https://doi.org/10.1016/j.jenvman.2007.06.009
3. Tchieno F.M.M., Tonle I.K. (2018) p-Nitrophenol determination and remediation: an overview, *Reviews in Analytical Chemistry, 37(2)*. https://doi.org/10.1515/revac-2017-0019
4. Din M.I., Khalid R., Hussain Z., Hussain T., Mujahid A., *et al.* (2020) Nanocatalytic assemblies for catalytic reduction of nitrophenols: a critical review, *Critical reviews in analytical chemistry, 50(4)*, 322-338. https://doi.org/10.1080/10408347.2019.1637241
5. Environmental Protection Agency U.S. (2014) Priority Pollutant List https://www.epa.gov/sites/default/files/2015-09/documents/priority-pollutant-list-epa.pdf (Accessed June 2021) .
6. Liu J., Li J., Meng R., Jian P., Wang L. (2019) Silver nanoparticles-decorated-Co_3O_4 porous sheets as efficient catalysts for the liquid-phase hydrogenation reduction of p-Nitrophenol, *Journal of colloid interface science, 551*, 261-269. https://doi.org/10.1016/j.jcis.2019.05.018
7. Guo Y., Dai M., Zhu Z., Chen Y., He H., *et al.* (2019) Chitosan modified Cu_2O nanoparticles with high catalytic activity for p-nitrophenol reduction, *Applied Surface Science, 480*, 601-610. https://doi.org/10.1016/j.apsusc.2019.02.246
8. Gu Y., Zhang Y., Zhang F., Wei J., Wang C., *et al.* (2010) Investigation of photoelectrocatalytic activity of Cu_2O nanoparticles for p-nitrophenol using rotating ring-disk electrode and application for electrocatalytic determination, *Electrochimica Acta, 56(2)*, 953-958. https://doi.org/10.1016/j.electacta.2010.09.051

accepted manuscript

9. Zhang S., Shang W., Yang X., Zhang S., *et al.* (2013) Immobilization of lipase using alginate hydrogel beads and enzymatic evaluation in hydrolysis of p-nitrophenol butyrate, *Bulletin of the Korean Chemical Society, 34(9)*, 2741-2746. https://doi.org/10.5012/bkcs.2013.34.9.2741
10. Liu J., Yan X., Wang L., Kong L., Jian P. (2017) Three-dimensional nitrogen-doped graphene foam as metal-free catalyst for the hydrogenation reduction of p-nitrophenol, *Journal of colloid interface science, 497*, 102-107. https://doi.org/10.1016/j.jcis.2017.02.065
11. Lu H., Yin H., Liu Y., Jiang T., Yu L. (2008) Influence of support on catalytic activity of Ni catalysts in p-nitrophenol hydrogenation to p-aminophenol, *Catalysis Communications, 10(3)*, 313-316. https://doi.org/10.1016/j.catcom.2008.09.015
12. Visibile A., Wang R.B., Vertova A., Rondinini S., Minguzzi A., *et al.* (2019) Influence of strain on the band gap of Cu_2O, Chemistry of Materials, 31(13), 4787-4792. https://doi.org/10.1021/acs.chemmater.9b01122
13. Zheng Z., Huang B., Wang Z., Guo M., Qin X., *et al.* (2009) Crystal faces of Cu_2O and their stabilities in photocatalytic reactions, *The Journal of Physical Chemistry C, 113(32)*, 14448-14453. https://doi.org/10.1021/jp904198d
14. Wang Z., Wang H., Wang L., Pan L. (2009) Controlled synthesis of Cu_2O cubic and octahedral nano-and microcrystals, *Crystal Research Technology: Journal of Experimental Industrial Crystallography, 44(6)*, 624-628. https://doi.org/10.1002/crat.200900136
15. Ahmed A., Gajbhiye N.S., Joshi A.G. (2011) Low cost, surfactant-less, one pot synthesis of Cu_2O nano-octahedra at room temperature, *Journal of Solid State Chemistry, 184*, 2209–2214. https://doi.org/10.1016/j.jssc.2011.05.058
16. Wang Y., Huang D., Zhu X., Ma Y., Geng H., *et al.* (2014) Surfactant-free synthesis of Cu_2O hollow spheres and their wavelength-dependent visible photocatalytic activities using LED lamps as cold light sources, *Nanoscale research letters, 9(1)*, 1-8. https://doi:10.1186/1556-276X-9-624
17. Yu Y., Du F.P., Jimmy C.Y., Zhuang Y., Wong P.K. (2004) One-dimensional shape-controlled preparation of porous Cu_2O nano-whiskers by using CTAB as a template, *Journal of Solid State Chemistry, 177(12)*, 4640-4647. https://doi.org/10.1016/j.jssc.2004.10.025

accepted manuscript

18. Naz G., Shamsuddin M., Butt F.K., Bajwa S.Z., Khan W.S., *et al.* (2019) Au/Cu_2O core/shell nanostructures with efficient photoresponses, *Chinese Journal of Physics, 59*, 307-316. https://doi.org/10.1016/j.cjph.2019.03.008
19. Xu C., Cao L., Su G., Liu W., Liu H., *et al.* (2010) Preparation of ZnO/Cu_2O compound photocatalyst and application in treating organic dyes, *Journal of hazardous materials, 176(1-3)*, 807-813. https://doi.org/10.1016/j.jhazmat.2009.11.106
20. Cheung R.C.F., Ng T.B., Wong J.H., Chan W.Y. (2015) Chitosan: an update on potential biomedical and pharmaceutical applications, *Marine drugs, 13(8)*, 5156-5186. https://doi.org/10.3390/md13085156
21. Kumari S., Kishor R. (2020) Handbook of Chitin Chitosan: Volume 1: Preparation Properties, 1st Ed., *Elsevier*, 1-33. https://doi.org/10.1016/C2018-0-03014-5
22. Divya K., Jisha M., (2018) Chitosan nanoparticles preparation and applications, *Environmental chemistry letters, 16(1)*, 101-112. doi: 10.1007/s10311-017-0670-y
23. Chen J.Y, Zhou P.J, Li J.L, Wang Y. (2008) Studies on the photocatalytic performance of cuprous oxide/chitosan nanocomposites activated by visible light, Carbohydrate Polymers, 72, 128-132. https://doi.org/10.1016/j.carbpol.2007.07.036
24. Cao C., Xiao L. (2014) Preparation and visible-light photocatalytic activity of Cu_2O/PVA/Chitosan composite films, *Advanced Materials Research, 1015*, 623-626. https://doi.org/10.4028/www.scientific.net/AMR.1015.623
25. Cao C., Xiao L., Liu L., Zhu H., Chen C., *et al.* (2013) Visible-light photocatalytic decolorization of reactive brilliant red X-3B on Cu_2O/crosslinked-chitosan nanocomposites prepared via one step process, *Applied Surface Science, 271*, 105-112. https://doi.org/10.1016/j.apsusc.2013.01.135
26. Ali M.E.A., Aboelfadl M.M.S., Selim A.M., Khalil H.F., Elkady G.M. (2018) Chitosan nanoparticles extracted from shrimp shells, application for removal of Fe(II) and Mn(II) from aqueous phases, *Separation Science Technology, 53(18)*, 2870-2881. https://doi.org/10.1080/01496395.2018.1489845
27. Sivakami M., Gomathi T., Venkatesan J., Jeong H., *et al.* (2013) Preparation and characterization of nano chitosan for treatment wastewaters, *International Journal of Biological Macromolecules, 57,* 204-212. https://doi.org/10.1016/j.ijbiomac.2013.03.005
28. Sasmal A.K., Dutta S., Pal T. (2016) A ternary Cu_2O-Cu-CuO nanocomposite: a catalyst with intriguing activity, *Dalton Transactions, 45(7)*, 3139-3150.

accepted manuscript

https://doi.org/10.1039/C5DT03859F

29. Mandlimath T.R., Gopal B. (2011) Catalytic activity of first row transition metal oxides in the conversion of p-nitrophenol to p-aminophenol, *Journal of Molecular Catalysis A: Chemical, 350(1-2)*, 9-15. https://doi.org/10.1016/j.molcata.2011.08.009
30. Zhang J., Yan Z., Fu L., Zhang Y., Yang H., *et al.* (2018) Silver nanoparticles assembled on modified sepiolite nanofibers for enhanced catalytic reduction of 4-nitrophenol, *Applied Clay Science, 166*, 166-173. https://doi.org/10.1016/j.clay.2018.09.026

accepted manuscript